INFECTION AND IMMUNITY, June 2005, p. 3210–3218 Vol. 73, No. 6
0019-9567/05/$08.00+0 doi:10.1128/IAI.73.6.3210–3218.2005

Role of Sialic Acid and Complex Carbohydrate Biosynthesis in Biofilm Formation by Nontypeable *Haemophilus influenzae* in the Chinchilla Middle Ear

Joseph Jurcisek,[1] Laura Greiner,[2] Hiroshi Watanabe,[2] Anthony Zaleski,[2] Michael A. Apicella,[2] and Lauren O. Bakaletz[1]*

Columbus Children's Research Institute and the College of Medicine & Public Health, The Ohio State University, Columbus, Ohio,[1] and The Department of Microbiology, The University of Iowa, Iowa City, Iowa[2]

Received 2 February 2005/Accepted 10 February 2005

Nontypeable *Haemophilus influenzae* (NTHI) is an important pathogen in respiratory tract infections, including otitis media (OM). NTHI forms biofilms in vitro as well as in the chinchilla middle ear, suggesting that biofilm formation in vivo might play an important role in the pathogenesis and chronicity of OM. We've previously shown that SiaA, SiaB, and WecA are involved in biofilm production by NTHI in vitro. To investigate whether these gene products were also involved in biofilm production in vivo, NTHI strain 2019 and five isogenic mutants with deletions in genes involved in carbohydrate biosynthesis were inoculated into the middle ears of chinchillas. The wild-type strain formed a large, well-organized, and viable biofilm; however, the *wecA*, *lsgB*, *siaA*, *pgm*, and *siaB* mutants were either unable to form biofilms or formed biofilms of markedly reduced mass, organization, and viability. Despite their compromised ability to form a biofilm in vivo, *wecA*, *lsgB*, and *siaA* mutants survived in the chinchilla, inducing culture-positive middle ear effusions, whereas *pgm* and *siaB* mutants were extremely sensitive to the bactericidal activity of chinchilla serum and thus did not survive. Lectin analysis indicated that sialic acid was an important component of the NTHI 2019 biofilm produced in vivo. Our data suggested that genes involved in carbohydrate biosynthesis and assembly play an important role in the ability of NTHI to form a biofilm in vivo. Collectively, we found that when modeled in a mammalian host, whereas biofilm formation was not essential for survivability of NTHI in vivo, lipooligosaccharide sialylation was indispensable.

Biofilms are aggregates of one or more types of bacteria attached to a biological or inert surface and encased in a glycocalyx or matrix. The biofilm matrix has many roles. It is thought to provide protection from environmental threats including antibiotics, surfactants, and host immune responses. The glycocalyx can also function as a scavenging system to trap and filter nutrients and essential minerals from the environment (9, 17, 21). This matrix is primarily comprised of bacterial exopolysaccharides and, in some cases, DNA, and it may contain host-derived proteins such as fibrinogen, fibronectin, and glycosaminoglycans (9, 17, 21, 26).

Nontypeable *Haemophilus influenzae* (NTHI) is an opportunistic pathogen that normally resides exclusively in the human nasopharynx as a commensal. NTHI can, however, cause acute otitis media (OM) and other respiratory tract illnesses and are the predominant pathogen in chronic OM. Recently, it has been shown that NTHI forms biofilms in vitro (16, 19) and in vivo (18, 19). Using a chinchilla model, Ehrlich et al. (11) demonstrated the presence of biofilms in animals inoculated with NTHI from 1 to 21 days after challenge. Fluorescent vital staining combined with confocal scanning laser microscopy (CSLM) showed that NTHI contained within the biofilms were viable. Collectively, these findings provide evidence that mucosal biofilms form in an experimental model of OM and suggest further that biofilm formation may be an important factor in the pathogenesis of chronic OM.

Our own recent studies indicate that genes involved in complex carbohydrate biosynthesis are involved in NTHI biofilm formation in vitro (12). To confirm that these same pathways are also operative in biofilm formation in vivo, in the present study we investigated the ability of NTHI strain 2019 and five isogenic deletion mutants to form a biofilm in the middle ear of the chinchilla host following direct challenge. Here we begin to define the role of SiaA, SiaB, Pgm, LsgB, and WecA in NTHI biofilm formation in vivo.

MATERIALS AND METHODS

Bacteria and culture conditions. Strains used are described in Table 1 (12). NTHI strain 2019 is a clinical isolate recovered from a patient with chronic obstructive pulmonary disease (5). This strain was reconstituted from a frozen stock culture and propagated at 37°C, 5% CO_2 on brain heart infusion (BHI) agar (Difco, Detroit, MI) supplemented with 10 μg hemin/ml (Sigma Chemical Co., St. Louis, MO) and 10 μg NAD/ml (Sigma).

Animal model. Eighteen adult chinchillas (*Chinchilla lanigera*) (three chinchillas [6 ears] per bacterial isolate) were used (mean weight, 400 to 600 g) (Rauscher's Chinchilla Ranch, LaRue, OH) after acclimation to the vivarium for a period of 7 to 10 days. Middle ears were inoculated with 300 μl sterile pyrogen-free saline containing 1,500 to 2,000 CFU NTHI, via transbullar (TB) inoculation as previously described (20), with the actual inoculum received confirmed by plate count. Middle ears were then monitored daily for signs of OM via video otoscopy and tympanometry. Due to the fact that mature biofilms are formed by NTHI in the chinchilla middle ear 5 days after challenge (11), in the present study chinchillas were also sacrificed at this time point, effusions (if present) were

* Corresponding author. Mailing address: Center for Microbial Pathogenesis, Columbus Children's Research Institute, Department of Pediatrics, The Ohio State University, College of Medicine and Public Health, 700 Children's Drive, Rm. W591, Columbus, OH 43205-2696. Phone: (614) 722-2915. Fax: (614) 722-2818. E-mail: BakaletL@pediatrics.ohio-state.edu.

TABLE 1. Bacterial strains

Strain	Genotype	Source or reference
NTHI 2019	Nontypeable *H. influenzae* wild type	14
NTHI 2019*lsgB*	Sialyltransferase mutant	14
NTHI 2019*pgm*	Phosphoglucomutase mutant	22
NTHI 2019*wecA*	Undecaprenyl-phosphate α-N-acetyl-glucosaminyltransferase mutant	12
NTHI 2019*siaA*	Sialyltransferase mutant	14
NTHI 2019*siaB*	CMP-Neu5Ac synthetase mutant	13

retrieved, and the bullae were removed. Bullae were then either snap frozen over liquid nitrogen and stored on dry ice or were packed on ice for immediate analysis of whole mounts using a vital fluorescent stain and CSLM. To compare the 36 challenged middle ears with those of a normal animal, an additional uninoculated chinchilla was sacrificed for recovery of bullae. Recovered effusions were serially diluted and plated for semiquantitative determination of CFU NTHI/ml middle ear fluid. All studies involving chinchillas were performed under an institutional Institutional Animal Care and Use Committee-approved protocol in compliance with all relevant federal guidelines and institutional policies.

Primary human bronchial airway epithelial cell cultures. Due to its unique phenotype in the chinchilla host (see Results), we further analyzed the ability of strain 2019*wecA* to form a biofilm when incubated with primary human bronchial epithelial cells. Briefly, cells were cultured on glass coverslips in 24-well plates as we have described previously (15). Infection was initiated by the addition of either 10^7 NTHI strain 2019 or 2019*wecA* (multiplicity of infection [MOI], ~100:1), followed by incubation for 72 h with medium changed after 24 h. To examine for biofilm formation, the glass coverslip was removed and placed in a well containing 4% glutaraldehyde, and the sample analyzed by scanning electron microscopy, as previously described (10).

Bactericidal assay. To determine whether the phenotype of no biofilm formation by two mutants, as observed in the chinchilla host, was perhaps due to increased sensitivity to complement-mediated killing by chinchilla serum, NTHI strain 2019 and all five isogenic deletion mutants were grown to early log phase, $A_{600} = 0.2$, in supplemented BHI broth. A 0.5-ml aliquot of each was centrifuged for 1 min at 10,000 × *g* (Eppendorf 54154 D centrifuge) at room temperature. The pellet was resuspended in 1.0 ml of phosphate buffered salt solution (PBSS) consisting of 10 mM K_2HPO_4, 10 mM KH_2PO_4, 136 mM NaCl, 5 mM KCl, 1 mM $CaCl_2$, 0.3 mM $MgCl_2$ $6H_2O$, 1 mM $MgSO_4$ $7H_2O$, and 0.01% bovine serum albumin (BSA), pH 7.0. A 1:10 dilution of this bacterial suspension was used to deliver approximately 10^5 bacteria to each well. The bactericidal assay, modified from that of Andreoni et al. (1), was carried out in a 96-well plate in a final volume of 200 μl, using pools of serum recovered from 3 or 4 adult chinchillas each that had been collected by centrifugation at 4°C from blood that was obtained aseptically by cardiac puncture. After allowing the blood to clot on ice, chinchilla serum was collected by centrifugation and immediately frozen and stored at −80°C until later use in this assay. The sensitivity of all strains to the bactericidal activity of chinchilla serum was assayed a minimum of three times on separate days.

LIVE/DEAD bacterial stain. Bullae that had previously been placed on ice were further dissected to isolate the inferior bullae, incubated with 30 μl of LIVE/DEAD stain (BacLight Bacterial viability kit; Molecular Probes, Eugene, OR) for 15 min, then rinsed in buffer. Biofilms were visualized using a Zeiss LSM510 META confocal scanning laser microscope (Carl Zeiss Microimaging Inc., Thornwood, NY).

Embedding in OCT for cryosectioning. To preserve the architecture of any biofilms that had formed in vivo, we embedded bullar mucosa in an optimal cutting temperature (OCT) compound (Fisher Scientific, Pittsburgh, PA) immediately after dissection for later cryosectioning. Briefly, the inferior and superior portions of iced, dissected bullae were separated, and any effusion present was retrieved by aspiration. The inferior bulla was then rinsed several times and drained via wicking onto absorbent paper. OCT was slowly added via 18-gauge needle. Bullae were then snap frozen over liquid nitrogen and placed on a bed of dry ice. External bone was carefully chipped away, thereby eliminating the need for decalcification as well as achieving our goal of leaving the middle ear mucosa and any attached biofilm intact. The resulting block was split in a plane perpendicular to the tympanic membrane. Serial sections (4 μm thickness) were cut on a Leica CM3050S cryotome (Leica Microsystems Inc., Bannockburn, IL), placed on Superfrost slides (Fisher Scientific, Pittsburgh, PA), fixed in 4% (wt/vol) paraformaldehyde (in 0.1 M phosphate buffer, pH 7.4) and stored at −80°C.

Lectin analysis. To characterize the NTHI strain 2019 biofilm by lectin analysis, OCT-embedded sections of a biofilm isolated from the chinchilla middle ear were cut into 4-μm-thick sections and incubated with the following lectins: *Maachia amurensis*-fluorescein isothiocyanate (MAA-FITC) and *Sambucus nigra*-Texas red isothiocyanate (SNA-TRITC) (both from EY Laboratories, San Mateo, California). *Maachia amurensis* lectin binds preferentially to a terminal Neu5Ac α2→3Gal, and *Sambucus nigra* lectin binds preferentially to terminal Neu5Ac α2→6Gal. Samples were examined by confocal microscopy, using a Bio-Rad CSLM located at the Central Microscopy Research Facility at the University of Iowa (Iowa City, IA).

Transmission electron microscopy (TEM). OCT sections were also processed for TEM by further embedding in LR White resin (Ted Pella, Inc., Redding, CA). Sections approximately 85 nm thick were cut, and the biofilm was then stained with 5% uranyl acetate for viewing with an H-7000 Hitachi transmission electron microscope.

RESULTS

Recent studies in our laboratory using in vitro assays show that NTHI strain 2019, strain 2019*pgm*, and strain 2019*lsgB* produce large biofilms with similar characteristics, while strains 2019*siaA*, strain 2019*siaB*, and strain 2019*wecA* produced significantly smaller amounts of biofilm (12). Here, we examined these strains in the chinchilla host to determine the potential impact of these mutations on biofilm formation in vivo. We found that whereas all ears showed some signs of inflammation during the 5-day observation period, the inflammatory response elicited by each of these six strains was highly variable, as was their ability to produce either an effusion (fluid) or form a biofilm in the middle ear space (Table 2).

Gross and microscopic morphology of the biofilms in situ. To grossly visualize any biofilm present and to qualitatively evaluate middle ears for signs of inflammation, chinchilla bullae were immediately imaged by stereomicroscope upon dis-

TABLE 2. Ears and NHTI

NTHI strain	No. of culture positive ears/ total ears inoculated	No. of ears in which a biofilm was observed upon gross dissection/ total ears inoculated with this strain	No. of ears on which CSLM was performed	No. of ears in which the presence of a biofilm was confirmed by CSLM/total no. ears reviewed	Mean % of bacteria in CSLM-confirmed biofilms that stained as viable cells (mean ± SD)	% strain surviving in in vitro bactericidal assay using chinchilla serum as a complement source (mean ± SD)
2019	6/6	6/6	4	4/4	100 ± 0	99.5 ± 4
2019*lsgB*	4/6	4/6	3	2/3	25 ± 7	85 ± 8
2019*siaA*	6/6	2/6	5	3/5	37 ± 46	80 ± 15
2019*wecA*	6/6	2/6	4	2/4	10 ± 0	98 ± 5
2019*siaB*	0/6	0/6	3	0/3	NA[a]	0 ± 0
2019*pgm*	0/6	0/6	5	1/5	90 ± 0	1 ± 3

[a] NA, not applicable.

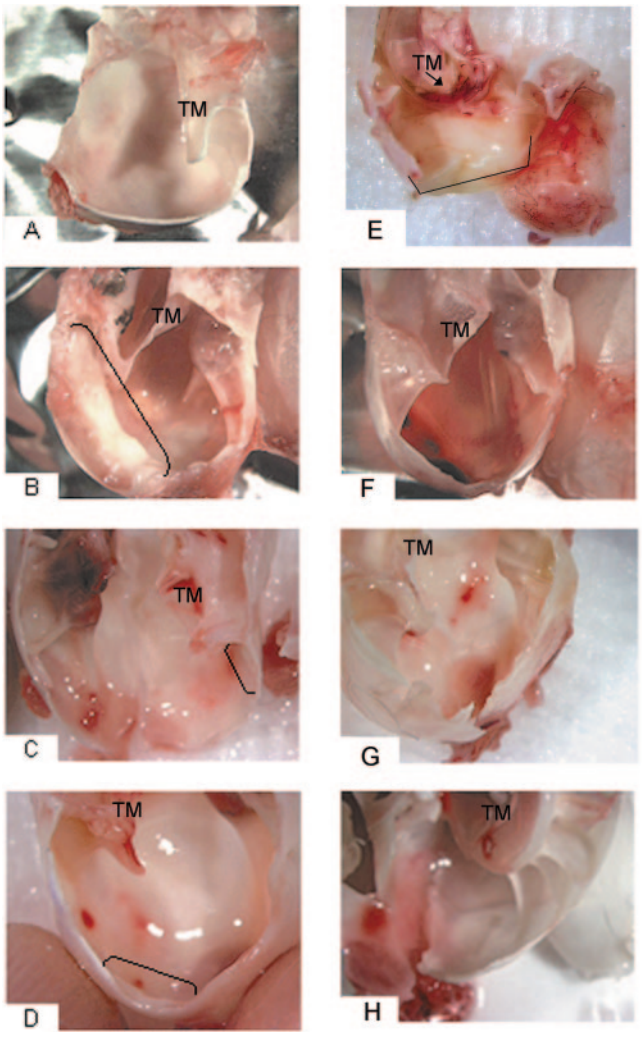

FIG. 1. Gross whole-mount images of bullae recovered 5 days postchallenge from chinchillas inoculated transbullarly with NTHI strain 2019 or a mutant derivative thereof. Brackets indicate biofilms (if present), and TM indicates tympanic membrane (or ear drum). (A) Bulla recovered from a naive chinchilla for comparison. Panel B shows large biofilm formed by strain 2019 in the chinchilla middle ear cavity 5 days after challenge. Strains 2019*lsgB* and 2019*siaA* (panels C and D, respectively) induced the formation of very small biofilms, easily identifiable only by stereomicroscopy. Strain 2019*wecA* formed a biomass in only two of the six challenged middle ears (panel E). In the remaining four middle ears, despite the presence of marked erythema, there were no discernible biomasses (panel F). Strains 2019*siaB* and 2019*pgm* (panels G and H, respectively) did not induce the formation of a biofilm that could be identified upon gross examination. Magnification all panels, 5×.

section. For reference, in a naive chinchilla the inferior bulla is comprised of thin bone lined by a shiny and colorless mucosal layer (Fig. 1A). The tympanic membrane is similarly thin and translucent in appearance with no signs of edema or erythema.

The bullae recovered from the chinchillas challenged with strain 2019 contained a large, creamy-colored and firm biofilm in the inferior aspect of the middle ear space in six of six ears (Table 2 and Fig. 1B). This biofilm extended along the bullar bone from approximately the tympanic orifice of the Eustachian tube to the bony niche immediately adjacent to the tympanic membrane. The biofilm formed by strain 2019 was easily seen by the naked eye and was of a consistent color and density throughout. The bone in the inferior bulla was opaque and thickened, suggesting that there had been considerable new bone formation. Mild erythema of the mucosal layer, with some blood vessel dilation, was also seen throughout the mucosa that lined the middle ear space.

Gross examination of the bullae recovered from chinchillas challenged with either 2019*lsgB* or 2019*siaA* (Fig. 1C and 1D, respectively) revealed very small biofilms in 4 of 6 and 2 of 6 ears, respectively, that could be seen clearly only with aid of the dissecting microscope. The biofilms produced by these latter two mutants were located along the ventral surface of the inferior bullae. The mucosa lining the bullae of these animals appeared less inflamed than that observed in the animal challenged with the parental strain (compare Fig. 1 panels C and D with panel B). Slight erythema was noted in these middle ears, with some focal hemorrhagic sites (most likely due to the epitympanic taps performed to retrieve middle ear fluids). However, overall the mucosal lining was shiny and did not appear to be edematous or grossly thickened. The bone of the inferior bulla was slightly more opaque in the animals challenged with 2019*siaA* than is typical for a naive animal; however, these changes were less marked than those noted in the middle ears of the animals challenged with the parent strain.

Mutant 2019*wecA* formed a grossly observable biomass in only 2 of 6 challenged middle ears (Table 2 and Fig. 1E and F). However, the bullae from the chinchillas challenged with the *wecA* mutant exhibited the greatest amount of erythema of all bullae examined in the present study (most easily seen in Fig. 1F). Overall, the erythema was rated as moderate in degree and was uniform across the inferior bulla, with several distinct hemorrhagic foci (again, likely induced by invasive epitympanic tapping). The bullar bone was thicker and more opaque than that of a naive animal; however, the tympanic membrane appeared normal overall.

The two remaining mutants studied here, 2019*siaB* and 2019*pgm* (Fig. 1G and 1H, respectively) did not form a biofilm in any of the six challenged middle ears of the chinchilla host, as evidenced by gross examination. The bullae recovered from chinchillas challenged with either 2019*siaB* or 2019*pgm* appeared highly similar to that of a naive animal, with the exception of areas of slight erythema throughout for the animals receiving strain 2019*siaB*.

To better characterize the biofilm created by the parent strain, we cryosectioned a mass that was adherent to the mucosa of the inferior bulla and analyzed it using both light microscopy of hematoxylin and eosin (H&E)-stained sections (Fig. 2A) or transmission electron microscopy (Fig. 2B). Strain NTHI 2109 produced a biofilm characterized by long fingerlike projections separated by what appeared to be numerous water channels (Fig. 2A, inset) (6, 7, 25). Electron microscopic analysis of an OCT- and Epon-embedded section of a characteristic biofilm produced by strain 2019 showed NTHI encased in a dense amorphous matrix (Fig. 2B).

Relative survival of NTHI strain 2019 and carbohydrate biosynthesis mutants in the chinchilla middle ear. At 5 days postchallenge, strain NTHI 2019 produced effusions in all six challenged chinchilla middle ears. These effusions yielded a mean of 3.4 E7 (±3 E7) CFU NTHI/ml (Fig. 3), which was

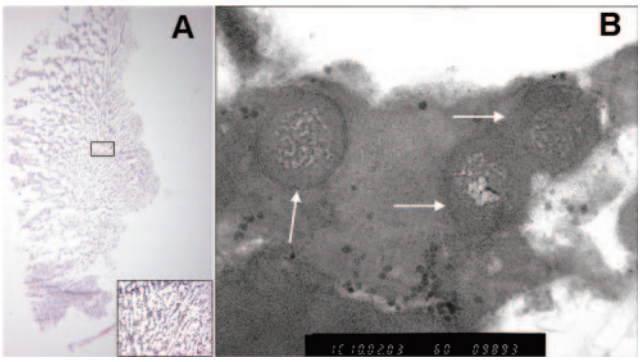

FIG. 2. (A) H&E stain of an OCT-embedded biofilm produced by strain 2019 in the chinchilla middle ear (5× magnification). Inset (100× magnification) clearly demonstrates what appears to be numerous water channels present within the biofilm. (B) TEM analysis of OCT-embedded biofilm formed by NTHI strain 2019 in the middle ear of a chinchilla. Arrows indicate bacteria surrounded by the biofilm matrix. This section was incubated with *Sambucus nigra* lectin conjugated to 15-nm gold beads. Note that the gold beads are seen bound to the biofilm matrix and not to the bacteria within the biofilm.

four logs greater than the challenge inoculum, indicating that this strain survived and multiplied within the chinchilla middle ears in this time period. Similarly, we obtained a mean count of 5.3 E7 (±1.1 E8) CFU NTHI/ml (Fig. 3) in effusions recovered from four of six ears challenged with strain 2019*lsgB* 5 days after inoculation. There were no effusions in the remaining two challenged middle ears (Table 2).

Whereas an effusion was recovered from three ears of the six challenged with either strain 2019*siaB* or with 2019*pgm*, at the time these effusions were recovered they were all sterile (i.e., there were no culturable bacteria within them) (Table 2 and Fig. 3). The remaining three ears in each of these latter two cohorts of animals had no effusions.

The final two mutants evaluated in the present study,

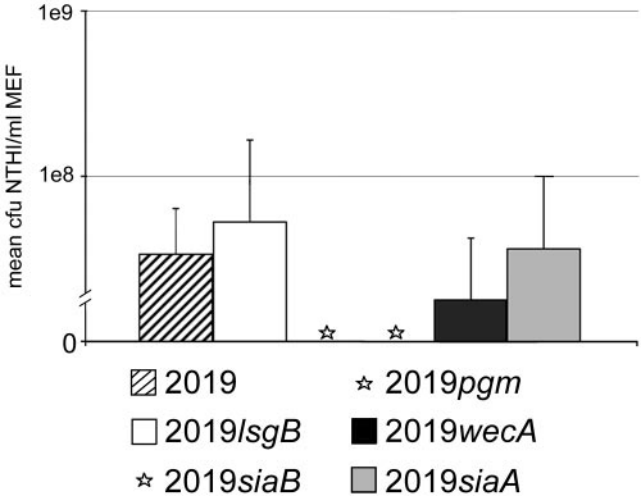

FIG. 3. Mean CFU NTHI per ml middle ear fluid (± standard deviations) as recovered from each of six middle ears challenged with either strain 2019 or one of its five deletion mutants. Strains 2019*siaB* and 2019*pgm* did not yield culture positive effusions in any of the six challenged middle ears (see asterisks in place of bars in figure).

2019*wecA* and 2019*siaA*, induced culture-positive effusions bilaterally in all three chinchillas (six ears each) (Table 2 and Fig. 3), as had the parental isolate, with CFU/ml counts that were several logs greater than the challenge inoculum (1.8 E7 ± 2.4 E7 and 3.7 E7 ± 6.3 E7, respectively), thus again demonstrating active growth in vivo.

In the situation in which there was no effusion in several of the challenged middle ears 5 days after inoculation (i.e., ears in cohorts of chinchillas challenged with strains 2019*lsgB*, 2019*siaB*, or 2019*pgm*), the data suggested that these mutants had been cleared from the middle ears more rapidly than the parental strain and were thus perhaps more sensitive to the chinchilla's immune response. Likewise, the presence of a sterile effusion 5 days after direct challenge of the middle ear space (i.e., ears in cohorts of chinchillas challenged with 2019*siaB* or 2019*pgm*) could indicate that either they too had ultimately been eradicated by host immune responses but had survived long enough to induce the formation of an effusion or perhaps that they were now exclusively occupying a biofilm within the tympanum and thus were not available for recovery in planktonic form for culture in vitro.

In vitro bactericidal assays conducted with chinchilla serum supported the concept of enhanced sensitivity to the chinchilla immune response for two of the five mutants characterized here (2019*siaB* and 2019*pgm*). Following a half-hour incubation in medium containing chinchilla serum, 99.5% of strain 2019, 98% of strain 2019*wecA*, 85% of strain 2019*lsgB*, and 80% of strain 2019*siaA* survived (Table 2). Conversely, only 1% of strain 2019*pgm* and none of strain 2019*siaB* could be recovered under the same conditions.

These latter two mutants were the only strains assayed in the present study that consistently induced either sterile effusions or no effusions in six of six challenged ears 5 days after challenge, whereas strain 2019*lsgB* induced culture positive effusions in four of six challenged ears and no effusions in the remaining two ears (Table 2). However, one of these latter two ears challenged with 2019*lsgB* was confirmed by CSLM examination to contain a densely packed and largely nonviable biofilm, suggesting that the absence of an effusion did not negate the possible existence of an NTHI-induced biofilm at some time point following direct challenge of the middle ear.

LIVE/DEAD fluorescent stain. To expand on observations made upon gross dissection, the contralateral bullae from each of the three chinchillas challenged with either strain 2019 or one of its five deletion mutants were stained with a vital fluorescent stain and viewed by confocal microscopy (Table 2 and Fig. 4).

Consistent with observations made of H&E-stained sections (see Fig. 2A), strain 2019 produced a well-defined and highly organized biofilm in the chinchilla middle ear that contained long finger-like projections with what appeared to be numerous water channels separating them (Fig. 4A) (6, 7, 25). These biofilms appeared to be comprised of viable NTHI (green fluorescence) throughout (Table 2). Collectively, our observations showed that strain 2019 could survive and multiply in the chinchilla host, but importantly they also demonstrated that this strain could consistently and reproducibly form a highly structured and viable biofilm in the middle ear space 5 days after challenge.

Despite our inability to visualize a biofilm grossly in any of

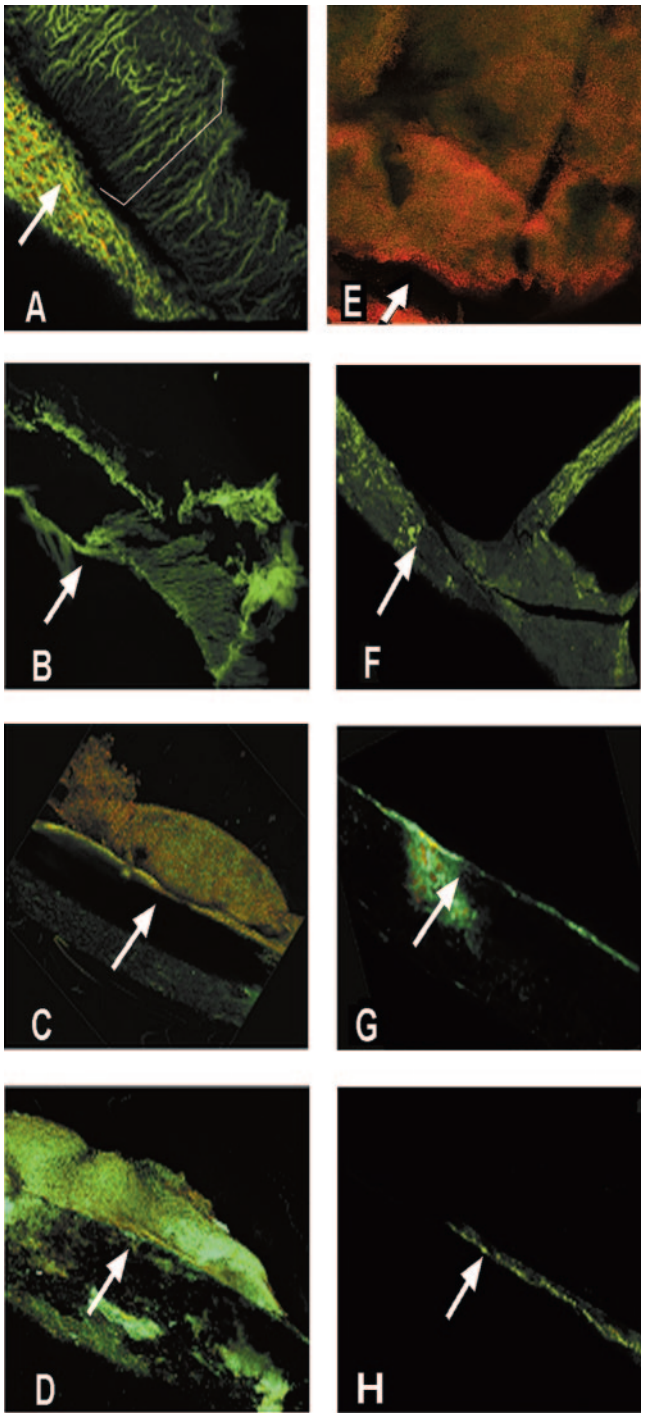

FIG. 4. Confocal microscopy images of whole-mount sections of chinchilla inferior bulla (white arrows indicate bone of the inferior bulla in each panel) stained with LIVE/DEAD bacterial stain 5 days after direct challenge with NTHI. The parent strain, 2019 (panel A) induced the formation of a large biofilm (white bracket) with long finger-like projections that appear to be separated by water channels that do not contain bacteria. These projections extend well into the middle ear space. Strain 2019*pgm* (panel B) formed a very small biofilm with what also appears to be water channels; however, this biofilm appeared to be less organized. Strains 2019*lsgB* (panel C) and 2019*siaA* (panel D) formed very dense biofilms with no apparent water channels. A much larger population of dead NTHI (red stain, panel C) was observed in the biofilm induced by strain 2019*lsgB* than seen in that produced by the parental isolate at this time point postchallenge of the six ears challenged with strain 2019*pgm*, when five of these biofilm-negative ears were further reviewed by CSLM, we were able to identify a very small biofilm present in one ear. The biofilm formed by this mutant in vivo (Fig. 4B) appeared to be comprised of ~90% viable NTHI. However, the biofilm produced by 2019*pgm* was notably smaller in size compared to that formed by strain 2019 in the same time period (compare Fig. 4A and B). In vitro, strain 2019*pgm* produces a biofilm that is highly similar in size and structure to that of the parental strain (12); however, since the biofilm produced by this mutant in the chinchillas was much smaller than that produced by the parent strain and because there were no culturable bacteria present in any of the middle ear fluids recovered at this time point, our data suggest enhanced sensitivity of this mutant to the host's immune response. As discussed above, this mutant was indeed highly susceptible to the bactericidal activity of chinchilla serum when assayed in vitro.

The mutation in *lsgB* also had an effect on the ability of this strain to produce a biofilm in vivo. Grossly, we observed a biofilm in four of six challenged middle ears. Upon further examination of two of these biofilm-positive ears (plus one of the ears that appeared negative for biofilm upon gross examination) by CSLM, we were able to confirm the presence of a biofilm in both ears that appeared positive for biofilm formation upon gross dissection. Both biofilms produced by strain 2019*lsgB* (Fig. 4C) had an architecture unlike that produced in vivo by NTHI strain 2019. These biofilms appeared to be very dense and compact with no apparent water channels. Moreover, there were large numbers of dead bacteria (≥70% nonviable) within the biofilm as demonstrated by the predominant red staining of NTHI due to uptake of propidium iodide. Overall, the fluorescent microscopy images supported the observations we made upon gross dissection of middle ears challenged with 2019*lsgB* (Fig. 1, panel C), wherein we reported evidence of a mild inflammatory response with limited new bone formation and the presence of only a very small biomass.

For the mutants 2019*siaA* and 2019*wecA*, despite the induction of culture-positive effusions, neither of these latter two mutants formed a biofilm that was similar architecturally to that formed by the parental strain, and in fact there was no evidence of a biofilm in four of six middle ears challenged with either 2019*siaA* or 2019*wecA* 5 days after challenge. Upon CSLM examination of one of the two ears of the 2019*siaA* middle ear. Strain 2019*wecA* induced the formation of a biomass in only two of the six challenged middle ears (panel E). These biomasses lacked architecture and were predominantly nonviable (bone of inferior bulla was viable; however, it appears black in this image because it was below the plane that was optimal for imaging the fluorescent bacterial biomass). In the majority of middle ears challenged with 2019*wecA*, there were no detectable biofilms; however, there were focal areas of bright fluorescence on the mucosal surface and the bone of the inferior bulla appears to be considerably thickened (panel F), suggesting the presence of viable bacteria and demonstrating that an inflammatory response, with new bone formation, had occurred following challenge of the depicted middle ear with strain 2019*wecA*. Strain 2019*siaB* (panel G) did not form detectable biofilms in the chinchilla middle ear 5 days after direct inoculation. A similarly stained naïve bulla is presented in panel H to demonstrate the normal thickness of the bone of the inferior bulla in an unchallenged chinchilla middle ear.

cohort that were positive for biofilm formation on gross observation plus an additional four ears that were negative for biofilm formation upon gross observation, we confirmed that there were no biofilms in two of these five ears. In the remaining three ears, the biofilms observed by CSLM were small and dense and had no visible water channels (Fig. 4D). Two of these biofilms were estimated as containing less than 10% viable bacteria, whereas the third appeared to be ~80 to 90% viable despite its extremely compact nature (this latter biofilm is depicted in panel D of Fig. 4).

Thus, strain 2019*siaA* formed biofilms in vivo that were very similar in structure to those produced by 2019*lsgB*, in that they were dense and compact and also appeared to lack the water channels present in the biofilm formed by the parental isolate. Since both of these latter two mutants induced the production of effusions that contained large numbers of viable, planktonic bacteria in either all or the majority of ears challenged, respectively, but were compromised in their ability to form biofilms similar to the parental isolate. Thereby, collectively our data suggest that the mutations in *siaA* and *lsgB* affected the ability of this organism to form an organized biofilm in vivo but did not either markedly decrease their overall fitness in vivo or greatly increase their sensitivity to the host's immune response.

The 2019*wecA* mutant also uniformly produced effusions containing large numbers of bacteria in all six challenged middle ears; however, biomasses were only observed grossly in two of these six middle ears (Fig. 4, panels E and F). Whereas the biomass induced following challenge with strain 2019 was characteristically firm in texture, that produced in two of the six ears challenged with 2019*wecA* was much softer in texture, had the consistency of uncooked egg white, and often streamed easily from the dissected bullae. Upon further examination of four 2019*wecA*-challenged middle ears by CSLM (two that were negative for biofilm formation upon gross examination and the two that were positive for the presence of a biofilm grossly), a biofilm was detected in the whole mounts stained with the vital fluorescent stain in only the two positive ears, thus again confirming the observations we made upon gross dissection. The biofilms observed were fairly large masses; however, they lacked defined architecture and were >90% nonviable (Fig. 4E and Table 2). Despite the absence of a biofilm in the remaining two ears challenged with 2019*wecA* when examined by CSLM (Fig. 4F), due to our observation of both thickened bone as well as what appeared to be focal areas of strong fluorescence on the mucosa lining these inferior bullae, we concluded that viable NTHI were likely adherent to the epithelial cells lining these middle ear spaces. To confirm this hypothesis, we conducted the scanning electron microscopy (SEM) study described below.

Finally, the enhanced sensitivity of strain 2019*siaB* to the chinchilla's immune response, as suggested by (i) data obtained in the bactericidal assay, (ii) the presence of sterile effusions in three of six challenged middle ears and no effusions in the remaining three ears 5 days after transbullar challenge, and (iii) the lack of biofilm formation in any of the six challenged ears as determined by gross visualization of dissected bullae (see Fig. 1) was further supported by fluorescent microscopy (Fig. 4G). There was no evidence of a biofilm in the middle ear space of any of the three ears examined by CSLM for this cohort of animals.

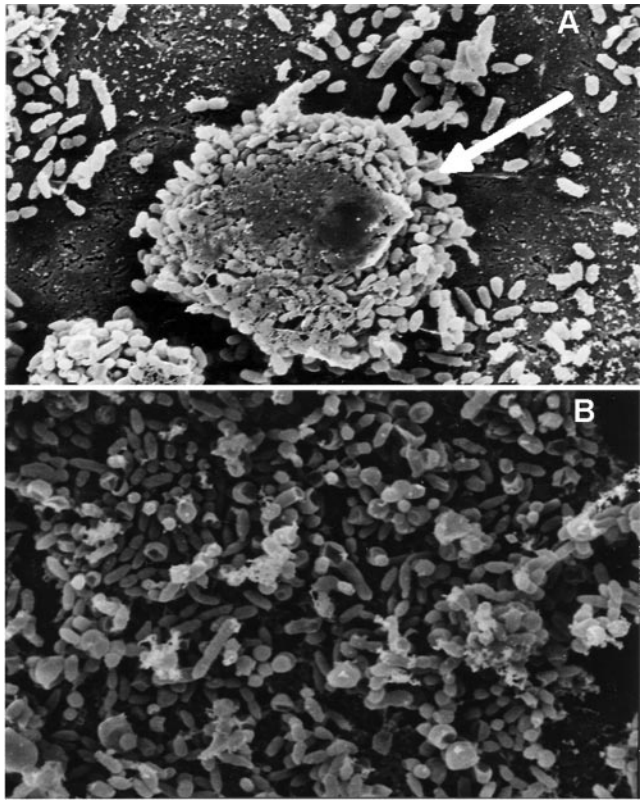

FIG. 5. SEM images of parent strain 2019 (panel A) and strain 2019*wecA* (panel B) incubated for 3 days on primary human bronchus cells. The parent strain formed organized microcolonies of bacteria (see arrow in panel A), whereas the mutant strain was seen to grow primarily as a monolayer of individual bacteria on the surface of these mucosal epithelial cells (panel B). The magnification of each panel is 6,000×.

The bulla of a naïve chinchilla, stained for confocal microscopy as those recovered from animals challenged with any of the above described NTHI strains, is depicted in Fig. 4H.

SEM analysis of strain 2019*wecA* infected human bronchial epithelial cells. We performed studies on strains 2019 and 2019*wecA* that had been allowed to infect primary human bronchial epithelial cells for a period of 72 h to determine if the characteristics of any biofilm induced by these strains in vitro were similar to those produced in vivo. Microcolonies and the initial formation of a biofilm can be seen with strain 2019 (Fig. 5A), whereas strain 2019*wecA* (Fig. 5B) formed neither structure and is instead seen as a monolayer of individual bacteria on the surface of the airway epithelial cells. These observations are very similar to the situation observed in chinchilla middle ears, wherein the parental isolate 2019 formed a well-organized biofilm in all challenged middle ears; however, the *wecA* mutant did not (compare Fig. 4A to E and F, respectively). The 2019*wecA* strain did, however, grow well in all six challenged middle ears and induced areas of strong fluorescence on the mucosal surface in the middle ear. Gross observations made on these dissected middle ears yielded multiple signs of inflammation.

Lectin analysis of the biofilm. The biofilm produced in the chinchilla middle ear by NTHI 2019 was further analyzed using

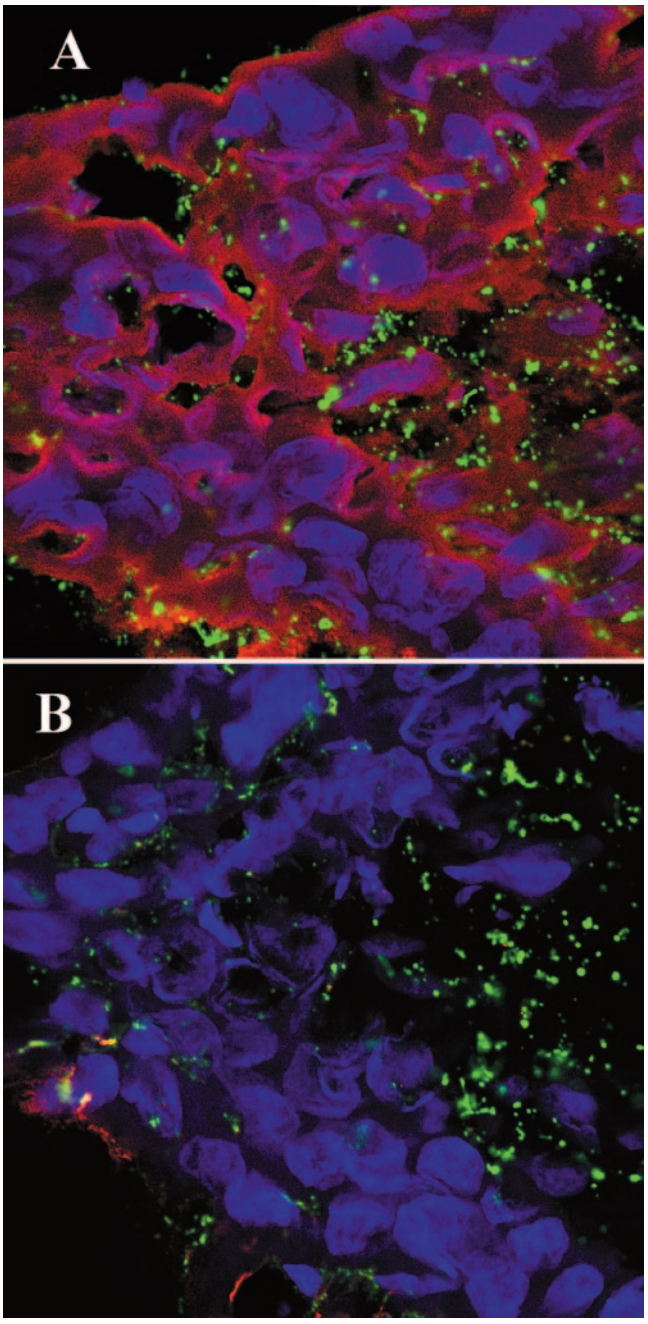

FIG. 6. Composite of confocal images obtained following incubation of an OCT-embedded biofilm produced by strain 2019 in the chinchilla middle ear with two fluorochrome-conjugated lectins. (A) Binding of the lectin *Sambucus nigra* (SNA-TRITC) is shown in red. The specificity of this lectin is for sialic acid α-2-6 galactose, and in these images it is shown binding to the biofilm matrix. *Macchia amurensia* lectin (MAA-FITC in green), which has specificity for sialic acid α-2-3 galactose and lactose, bound to the LOS of the NTHI present within the biofilm. (B) Lectin labeling obtained after neuraminidase treatment of a serial section of the same OCT-embedded biofilm that is shown in panel A. Neuraminidase removed labeling by SNA-TRITC of the biofilm completely, confirming the presence of sialic acid in an α-2-6 linkage within the biofilm matrix (4). There was minimal change observed in the binding of MAA-FITC to NTHI within the biofilm after neuraminidase treatment. In addition, these sections show the infiltration of the biofilm by inflammatory cells (the nuclei of which are labeled blue with a DNA stain [To-Pro3]). The magnification of each panel is 1,200×.

two lectins. The *Sambucus nigra* lectin (SNA) preferentially binds Neu5Acα2→6galactose, and *Maachia amurensis* lectin (MAA) preferentially binds Neu5Acα2→3galactose. Analysis by CSLM indicated that SNA conjugated to TRITC (SNA-TRITC) bound to the 5-acetylneuraminic acid (Neu5Ac) in the biofilm matrix, whereas MAA conjugated to FITC (MAA-FITC) bound to the Neu5Ac and lactosyl groups on the LOS of NTHI within the biofilm matrix (Fig. 6A). To confirm that the labeling observed was in fact due to the presence of sialic acid, an adjacent serial section of the same biofilm was treated with neuraminidase prior to lectin labeling. Neuraminidase removed essentially all of the labeling by SNA-TRITC and some of the binding of MAA-FITC to the biofilm (Fig. 6B). Additionally, it appeared that SNA-TRITC now bound diffusely to the biofilm matrix while the MAA-FITC bound exclusively to the organisms within the biofilm. This latter lectin has specificity for lactose as well as sialic acid, while SNA shows specificity for sialic acid in an α2-6 linkage (4). Thereby, these data suggested that the sialic acid contained within the NTHI 2019 biofilm matrix induced in vivo is in an α2-6 linkage, in contrast to the α2-3 linkage known to be present within LOS expressed by NTHI 2019 (14). These sections were also stained with the DNA stain To-Pro3, which revealed the nuclei of numerous monocytic-like host cells that appeared to be infiltrating the biofilm.

DISCUSSION

A biofilm matrix is primarily comprised of bacterial exopolysaccharides, along with components scavenged from the environment. NTHI produces LOS and often decorates its LOS with sialic acid that has been acquired from its host. Sialic acid on the surface of bacteria is thought to confer resistance to both complement-mediated killing and the ability to bind to host cell receptors. NTHI has three distinct sialyltransferases, SiaA, Lic3A, and LsgB (14), all of which can be involved in placing sialic acid on the LOS. SiaA has homology to a sialyltransferase identified in *H. ducreyi* and utilizes a terminal lactosamine (Gal-GlcNAc) as an acceptor. Lic3A is an α-2,3-sialytransferase, with homology to the sialyltransferase in *Campylobacter jejuni*, and it uses a terminal Gal-Gal as an acceptor. LsgB places sialic acid on a terminal lactosamine of the LOS but differs from the acceptor of SiaA by the presence of a unique substitution on lactosamine. We have shown that SiaA is the sialyltransferase involved in incorporating sialic acid into the biofilm (23). For NTHI, sialic acid is obtained from environmental sources of 5-acetylneuraminic acid (Neu5Ac). Prior to transfer to LOS, the sialic acid must first be activated by the addition of a CMP group (cystidine-5-phosphate) (23, 24). The gene responsible for this activity encodes a CMP-NANA synthase (SiaB). After activation, sialic acid is then transferred, via a sialyltransferase, as a terminal structure onto the LOS (24).

We have also identified genes responsible for carbohydrate biosynthesis that have a high probability of being involved in biofilm formation by NTHI (12). A mutation in the gene that encodes UDP-GlcNAc:undecaprenylphosphate GlcNAc-1-phosphate transferase (*wecA*) results in markedly reduced biofilm formation in vitro. The gene product of *wecA* adds the first sugar to the carrier lipid undecaprenol in the biosynthesis

of complex carbohydrates such as bacterial common antigen and O-antigens. WecA is not involved in NTHI LOS biosynthesis but appears to be involved in the synthesis of the biofilm polymer. Thus, our studies to date suggest that a crucial component of the biofilm is assembled on a carrier lipid and then transported to the external environment. Phosphoglucomutase, a homolog to AlgC of *Pseudomonas aeruginosa*, shown to have a central role in the production of alginate and lipopolysaccharide, is an enzyme responsible for the conversion of glucose-6-phosphate to glucose-1-phosphate. In carbohydrate biosynthesis, glucose-1-phosphate is further converted to UDP-glucose and/or UDP-galactose. These nucleotide sugars are then used as substrates for incorporation of hexoses into the complex carbohydrates. Mutation in *pgm* abrogates this process due to nucleotide substitution of these hexoses (23).

Previously, NTHI strain 2019 and deletion mutants constructed in the genes listed above were analyzed for their ability to form biofilms in vitro (12) using both flow chambers as well as primary human bronchus cell cultures (15). Here, we used a chinchilla transbullar challenge model (3, 20) to now study the ability of strain 2019 and several of these mutants to form biofilms in a mammalian host, as have been described for other strains of NTHI (2, 11). Moreover, we analyzed the glycocalyx of the biofilm produced in vivo using lectin labeling. We found that all five isolates with deletion mutations within genes involved in LOS biosynthesis were compromised in their ability to survive and/or form a mature biofilm in the chinchilla middle ear. Whereas the parental strain NTHI 2019 was able to multiply within the tympanum, induce culture-positive effusions, and form large, viable, and well-organized biofilms, isolates with mutations in the sialyltransferase *lsgB* or *siaA* showed a markedly different phenotype. When strain 2019*lsgB* was inoculated into chinchilla middle ears, when present the biofilm produced was dense and contained a large proportion of dead bacteria. Culture positive effusions were present in four of six middle ears challenged with this mutant. Conversely, strain 2019*siaA* survived and multiplied, producing effusions in all six challenged middle ears. However, like the *lsgB* mutant, this isolate produced a biofilm in only approximately half the challenged middle ears. Moreover, the biofilm produced was dense, with no evident water channels, and was comprised primarily of nonviable bacteria. Thereby, while clearly both 2019*siaA* and 2019*lsgB* survived long enough in several of the challenged middle ears to induce the formation of a biofilm, by 5 days after inoculation the biofilms produced were atypical of that formed by the parental isolate and, unlike that of strain 2019, the biofilms formed by either 2019*siaA* or 2019*lsgB* contained predominantly nonviable NTHI.

NTHI strain 2019*wecA* also survived and multiplied well within the chinchilla middle ear, producing culture-positive effusions in all six challenged middle ears; however, we were unable to detect the presence of a biofilm in four of these six middle ears by any method used. In the two ears in which a biomass was observed grossly, it was of a much softer consistency than that produced by the parental isolate. When further characterized by CSLM, in combination with a fluorescent vital stain, these biofilms lacked characteristic architecture, and ~90% of the bacteria contained within them were nonviable. This mutation likely interrupts the first step in biofilm biosynthesis, thus the phenotype is either a complete loss of or significantly reduced biofilm production, as we reported in the in vitro flow chamber assays (12) and now corroborate here, in an animal model.

Strain 2019*pgm*, with a deletion in a phosphoglucomutase gene, did not survive as well as the parental isolate within the middle ear. At 5 days postinoculation, the effusions recovered from three of the challenged middle ears were sterile, and there were no effusions in the remaining three ears. Prior to sacrifice, this latter strain did,however, induce the formation of a biofilm in one of the six challenged chinchilla middle ears. By CSLM, we observed that this biofilm, while comprised of ~90% viable NTHI, was significantly smaller and less well organized than that produced by the parental isolate. The fifth mutant assayed, NTHI 2019*siaB*, was deficient in its ability to express a CMP-NANA synthetase. Direct inoculation of the chinchilla middle ear with this isolate resulted in the formation of a sterile effusion in three of six challenged middle ears and no effusion in the remaining three ears. There was no evidence of a biofilm 5 days after inoculation in any of the six middle ears.

Data we obtained with 2019*siaB* are consistent with those of Swords et al. (23), who assayed this mutant for survivability in a gerbil middle ear challenge model and also found that it was significantly compromised in ability to colonize and persist in vivo. Whereas we found sterile middle ear effusions in three of six ears 5 days after challenge, Swords and colleagues were able to recover NTHI, albeit at greatly reduced concentrations compared to the inoculum, from the gerbil middle ears up to 3 days postinoculation. These differences are likely due to both the interval between direct challenge and sample collection as well as the large difference in inocula used (~2,000 versus 10^7 CFU for chinchillas and gerbils, respectively). Whereas sensitivity to gerbil complement-mediated killing was not reported for the *siaB* mutant in that study (23), it greatly enhanced sensitivity to chinchilla serum relative to the parent isolate was shown here and likely played a key role in our observations.

In summary, we assayed the wild-type strain NTHI 2019 and five isogenic mutants for their ability to form a biofilm in vivo and compared these findings to their ability to do so in vitro. Overall, we found good correlation between the in vitro and in vivo findings. However, in the chinchilla model, the presence of an intact host immune system likely contributed to the observed compromised survivability of, and in ability to form a biofilm by, strains 2019*lsgB*, 2019*siaB*, and 2019*pgm.* These latter two mutants were both highly susceptible to complement-mediated bactericidal activity of chinchilla serum in vitro. Our studies also indicated that a *wecA* mutant behaved in a similar manner on human airway epithelial cells in culture and in the chinchilla middle ear. Infection in both models persisted for the duration of the experiments, but there was failure to form microcolonies or an organized, viable biofilm, respectively.

We are confident that the phenotype of these mutants observed in vivo is attributable to the mutations made and not due to a polar effect for the following reasons. For strain 2019*wecA*, there are 800 bp between it and the upstream gene (HI1716), which is transcribed in the opposite direction. For the sialyltransferase mutants 2019*lsgB* and 2019*siaA*, these mutant constructs have been shown not to have a polar effect on downstream genes in the operon (14). In strain 2019*pgm*, the 3′ end of the deleted gene (HI0740) is 160 bp from the 5′ end of

the upstream gene. There is no polar effect on HI0741 by the mutation in *pgm* (22). Finally, strain 2019*siaB*, there are 1,593 bp between the 3′ end of *pgm* and the 5′ end of the upstream gene (HI1280). Moreover, whereas all of the five mutants characterized here were shown to be either incapable of inducing a biofilm in vivo or produced a biofilm with a very altered architecture and viability profile, other mutants constructed in the strain 2019 genetic background are unaffected in terms of their ability to form a biofilm in the middle ears of the chinchilla host. Strains with mutations in *rfaD* and *htrB* have been tested in chinchillas previously (8). While this early study predates investigations that focused on the role of biofilms in otitis media, the authors reported that whereas the *rfaD* mutant was rapidly cleared from the middle ears of this rodent host, the *htrB* mutant persisted for up to 5 weeks after challenge in those cohorts that received the two higher of three doses tested. Also, in as-yet unpublished observations from our laboratories, we have shown that a deletion mutation in *lsgG* (a *lysR* type regulator) had no effect on the ability of strain 2019 to form a biofilm in vivo in the chinchilla middle ear.

In an intact biological model system, such as when modeling experimental OM in the chinchilla middle ear, the interactions between bacterial virulence factors and host defenses can be analyzed. From these studies, it is clear that global effects on sialylation (*siaA*, *siaB*, and *lsgB* mutants) of both LOS and the biofilm alter the ability of the organism to survive in a mammalian host. Modifications that effect biofilm formation alone, such as mutation in *wecA*, appear to have less of an effect on the organism's persistence in vivo despite its marked influence on ability to form a viable organized biofilm on a mucosal surface in the uppermost airway of an intact mammalian host. It would appear from this work, and that of others, that biofilm formation occurs during infection in vivo; however, here we showed that whereas biofilm formation was not essential for bacterial survival in the chinchilla middle ear, LOS sialylation was indispensable. Moreover, sialic acid appeared to be incorporated into the biofilm matrix that was produced by NTHI in vivo.

ACKNOWLEDGMENTS

This work was supported by grant R01-DC0391 to L.O.B. from NIDCD/NIH and grants AI30040 and AI24616 to M.A.A. from NIAID/NIH.

We thank Jennifer Neelans for manuscript preparation.

REFERENCES

1. **Andreoni, J., H. Kayhty, and P. Densen.** 1993. Vaccination and the role of capsular polysaccharide antibody in prevention of recurrent meningococcal disease in late complement component-deficient individuals. J. Infect. Dis. **168:**227–231.
2. **Bakaletz, L. O., B. D. Baker, J. A. Jurcisek, H. Harrison, L. A. Novotny, J. E. Bookwalter, R. Mungur, and R. S. Munson, Jr.** Demonstration of type IV pilus expression and a twitching phenotype by *Haemophilus influenzae.* Infect. Immun., in press.
3. **Bakaletz, L. O., B. J. Kennedy, L. A. Novotny, G. Duquesne, J. Cohen, and Y. Lobet.** 1999. Protection against development of otitis media induced by nontypeable *Haemophilus influenzae* by both active and passive immunization in a chinchilla model of virus-bacterium superinfection. Infect. Immun. **67:**2746–2762.
4. **Brinkman-Van der Linden, E. C., J. L. Sonnenburg, and A. Varki.** 2002. Effects of sialic acid substitutions on recognition by *Sambucus nigra agglutinin* and *Maackia amurensis* hemagglutinin. Anal. Biochem. **303:**98–104.
5. **Campagnari, A. A., M. R. Gupta, K. C. Dudas, T. F. Murphy, and M. A. Apicella.** 1987. Antigenic diversity of lipooligosaccharides of nontypable *Haemophilus influenzae*. Infect. Immun. **55:**882–887.
6. **Chang, W. S., and L. J. Halverson.** 2003. Reduced water availability influences the dynamics, development, and ultrastructural properties of *Pseudomonas putida* biofilms. J. Bacteriol. **185:**6199–6204.
7. **Costerton, J. W., Z. Lewandowski, D. E. Caldwell, D. R. Korber, and H. M. Lappin-Scott.** 1995. Microbial biofilms. Annu. Rev. Microbiol. **49:**711–745.
8. **DeMaria, T. F., M. A. Apicella, W. A. Nichols, and E. R. Leake.** 1997. Evaluation of the virulence of nontypeable *Haemophilus influenzae* lipooligosaccharide *htrB* and *rfaD* mutants in the chinchilla model of otitis media. Infect. Immun. **65:**4431–4435.
9. **Dunne, W. M., Jr.** 2002. Bacterial adhesion: seen any good biofilms lately? Clin. Microbiol. Rev. **15:**155–166.
10. **Edwards, J. L., J. Q. Shao, K. A. Ault, and M. A. Apicella.** 2000. *Neisseria gonorrhoeae* elicits membrane ruffling and cytoskeletal rearrangements upon infection of primary human endocervical and ectocervical cells. Infect. Immun. **68:**5354–5363.
11. **Ehrlich, G. D., R. Veeh, X. Wang, J. W. Costerton, J. D. Hayes, F. Z. Hu, B. J. Daigle, M. D. Ehrlich, and J. C. Post.** 2002. Mucosal biofilm formation on middle-ear mucosa in the chinchilla model of otitis media. JAMA **287:**1710–1715.
12. **Greiner, L. L., H. Watanabe, N. J. Phillips, J. Shao, A. Morgan, A. Zaleski, B. W. Gibson, and M. A. Apicella.** 2004. Nontypeable *Haemophilus influenzae* strain 2019 produces a biofilm containing N-acetylneuraminic acid that may mimic sialylated O-linked glycans. Infect. Immun. **72:**4249–4260.
13. **Hood, D. W., M. E. Deadman, T. Allen, H. Masoud, A. Martin, J. R. Brisson, R. Fleischmann, J. C. Venter, J. C. Richards, and E. R. Moxon.** 1996. Use of the complete genome sequence information of *Haemophilus influenzae* strain Rd to investigate lipopolysaccharide biosynthesis. Mol. Microbiol. **22:**951–965.
14. **Jones, P. A., N. M. Samuels, N. J. Phillips, R. S. Munson, Jr., J. A. Bozue, J. A. Arseneau, W. A. Nichols, A. Zaleski, B. W. Gibson, and M. A. Apicella.** 2002. *Haemophilus influenzae* type B strain A2 has multiply sialytransferases involved in lipo-oligosaccharide sialylation. J. Biol. Chem. **277:**14598–14611.
15. **Ketterer, M. R., J. Q. Shao, D. B. Hornick, B. Buscher, V. K. Bandi, and M. A. Apicella.** 1999. Infection of primary human bronchial epithelial cells by *Haemophilus influenzae*: macropinocytosis as a mechanism of airway epithelial cell entry. Infect. Immun. **67:**4161–4170.
16. **Murphy, T. F., and C. Kirkham.** 2002. Biofilm formation by nontypeable *Haemophilus influenzae*: strain variability, outer membrane antigen expression and role of pili. BMC Microbiol. **2:**7.
17. **O'Toole, G., H. B. Kaplan, and R. Kolter.** 2000. Biofilm formation as microbial development. Annu. Rev. Microbiol. **54:**49–79.
18. **Post, J. C.** 2001. Direct evidence of bacterial biofilms in otitis media. Laryngoscope **111:**2083–2094.
19. **Rayner, M. G., Y. Zhang, M. C. Gorry, Y. Chen, J. C. Post, and G. D. Ehrlich.** 1998. Evidence of bacterial metabolic activity in culture-negative otitis media with effusion. JAMA **279:**296–299.
20. **Sirakova, T., P. E. Kolattukudy, D. Murwin, J. Billy, E. Leake, D. Lim, T. DeMaria, and L. Bakaletz.** 1994. Role of fimbriae expressed by nontypeable *Haemophilus influenzae* in pathogenesis of and protection against otitis media and relatedness of the fimbrin subunit to outer membrane protein A. Infect. Immun. **62:**2002–2020.
21. **Sutherland, I. W.** 2001. The biofilm matrix–an immobilized but dynamic microbial environment. Trends Microbiol. **9:**222–227.
22. **Swords, W. E., B. A. Buscher, K. Ver Steeg II, A. Preston, W. A. Nichols, J. N. Weiser, B. W. Gibson, and M. A. Apicella.** 2000. Non-typeable *Haemophilus influenzae* adhere to and invade human bronchial epithelial cells via an interaction of lipooligosaccharide with the PAF receptor. Mol. Microbiol. **37:**13–27.
23. **Swords, W. E., M. L. Moore, L. Godzicki, G. Bukofzer, M. J. Mitten, and J. VonCannon.** 2004. Sialylation of lipooligosaccharides promotes biofilm formation by nontypeable *Haemophilus influenzae*. Infect. Immun. **72:**106–113.
24. **Vimr, E., and C. Lichtensteiger.** 2002. To sialylate, or not to sialylate: that is the question. Trends Microbiol. **10:**254–257.
25. **Wentland, E. J., P. S. Stewart, C. T. Huang, and G. A. McFeters.** 1996. Spatial variations in growth rate within *Klebsiella pneumoniae* colonies and biofilm. Biotechnol. Prog. **12:**316–321.
26. **Wozniak, D. J., T. J. Wyckoff, M. Starkey, R. Keyser, P. Azadi, G. A. O'Toole, and M. R. Parsek.** 2003. Alginate is not a significant component of the extracellular polysaccharide matrix of PA14 and PAO1 *Pseudomonas aeruginosa* biofilms. Proc. Natl. Acad. Sci. USA **100:**7907–7912.

Editor: D. L. Burns